NOISE SOURCES IDENTIFICATION ON A LARGE STAMPING PRESS

Pérecles Costa Azevedo
Rua Suíça 49A – 32.340-090 – Contagem – MG - Brazil
pereclesazevedo@hotmail.com

ArcanjoLenzi
UFSC – Cx. Postal 476 – 88.040-900 – Florianópolis – SC - Brazil
arcanjo@emc.ufsc.br

Roberto Jordan
UFSC – Cx. Postal 476 – 88.040-900 – Florianópolis – SC - Brazil
jordan@emc.ufsc.br

Abstract. *This paper presents an analysis of the noise emitted by a large eccentrical stamping press. A time history analysis is performed in order to identify the noisiest phases of the stamping process. A set of noise spectra, obtained along a complete cycle of the press, helps to analyze the frequency contents of the noise signal. Sound power levels of several press components are estimated and ranked, making it possible the identification of the main noise sources. These estimated sound power levels are then used to calculate the sound pressure level at operator's position, which is compared to experimental results. From the time analysis, it is concluded that the critical moments are those when the hammer impacts and fractures the material. Estimated sound power levels show that the main continuous noise sources are the the press head areas, the hammer and the electrical motor. It was also concluded that impact noise is mainly produced by the fast hammer deceleration and material fracture. Finally, good agreement between estimated and measured sound pressure levels, at operator's position, shows that the applied hypothesis on sound radiation estimation are quite reasonable.*

Keywords*: noise analysis, punch press, sources identification*

1. Introduction

High impact noise pressure levels are produced by eccentrical presses under operation. Each time the press hammer is activated and hits the metal sheet, a large amount of energy is released. The stamping process is intrinsically noisy, and radiates large amounts of sound energy directly to the surrounding areas. The energy release causes also a great amount of structural vibrations, which in turn is responsible for additional sound production. Other press elements like motors, clutch and brake also generate noise (Stimpson and Richards, 1985). The noise produced during the whole stamping process is investigated.

2. Press characteristics

The press under investigation is of an eccentric mechanical type, with characteristics as presented at Tab. 1. The maximum force value is obtained at 12.5 mm from the lower limit point of displacement.

Table 1: Characteristics of the press.

Maximum force	810 ton
Hammer dimensions (width x depth)	4.57 m x 2.46 m
Punches/min	16
Maximum height	10 m
Main motor electrical power	90 kW

2. Time history analysis

A first approach to investigate the stamping noise production was through the analysis of time history signals (Azevedo, 2003). As an example, it is shown in Fig. 1 the noise signal obtained by a microphone at 1 m from the press, in its front region, 1.5 m above floor.

From Fig. 1, six sequential phases were identified and named as: A-B) hammer downward acceleration; B-C) hammer descent; C-D) hammer impact; D-E) material fracture; E-F-G-H) hammer ascend; H-I) hammer deceleration and stop. The main noise phenomena are hammer impact and material fracture, whose noise levels are approximately 16 dB higher than the levels presented by other phases.

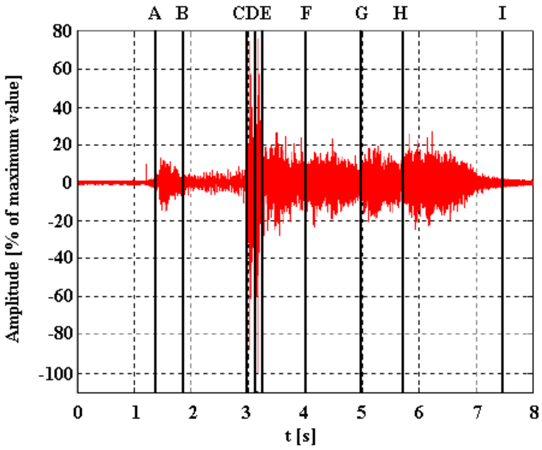

Figure 1: Noise time history signal acquired in front of press, for a complete cycle operation.

It can be seen, from Fig. 1, that the noisiest phases are hammer impact (C-D) and material fracture (D-E). The following period (E-H) is characterized by high structure vibration levels, as a consequence of the hammer impact, and the noise emission is of considerable amount. Deceleration and braking of the hammer (H-I) also produce noise; level values are equivalent to those of the preceding phase. The noise observed at the initial phase (hammer acceleration - A-B), although of easy perception, presents lower level value.

To obtain useful noise levels from time history signals, it was used a procedure based on one third octave filtering and time averaging. Time averaging used two different RC circuits, with 35 ms time constants (leading to fast linear values – SPL_{35ms}) and 1 s (leading to slow dBA values, after the A-weighting curve correction factors were applied to the resulting values – SPL_{1s}). The resulting values, corresponding to all phases and to the background noise, are presented at Tab. 2.

Table 2: Noise levels during press operation.

	Background noise	Phases							
		A-B	B-C	C-D	D-E	E-F	F-G	G-H	H-I
SPL_{35ms} [dB]	92	100	95	120	118	105	105	105	98
SPL_{1s} [dBA]	69	88	87	91	97	100	94	94	95

3. Frequency analysis

The spectra of the noise of the same signal presented in the former section are now analyzed over a complete cycle. The results are shown in Figs. 2 and 3, for SPL_{35ms} and SPL_{1s} values. These spectra show noise levels in one third octave bands, with central frequencies from 20 Hz to 3,150 Hz. The lines of same sound pressure are 6 dB apart (Azevedo, 2003).

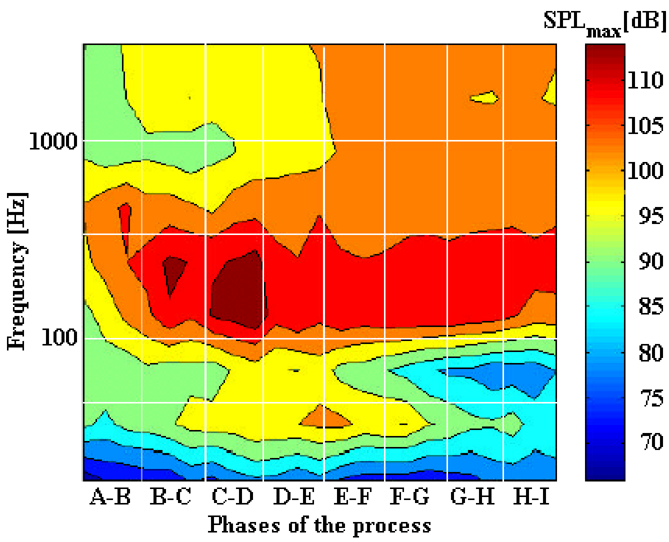

Figure 2: Spectra of SPL_{35ms} along one punch cycle.

From Fig. 2 it is possible to conclude that the noise energy is mainly concentrated at low frequencies (100 Hz to 500 Hz) and that the maximum impulsive levels occur at phase C-D, reaching values up to 120 dB. Analysis of Fig. 3 shows that the equivalent noise presents high values all through the frequency range, from 50 Hz to 3,000 Hz.

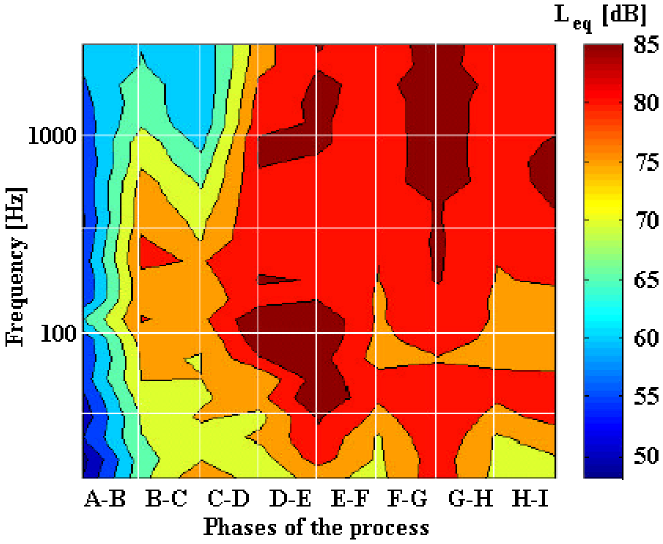

Figure 3: Spectra of SPL_{1s} along one punch cycle.

4. Sound power estimation

To help the identification of the main noise sorces, the total noise was divided into several contributions, that were related to the following components (with exception of first and last components):

S1 – wood floor near press;
S2 – base;
S3 – lower stamp;
S4 – hammer;
S5 – frontal head area;
S6 – lateral head area;
S7 – lower cover sheets;
S8 – upper cover sheets;
S9 – lateral protection cover sheets;
S10 – pieces convey;
S11 – main electric motor;
S12 – clutch system;
S13 – brake system;
S14 – material fracture, stamps direct impact and air expulsion during stamping.

Figures 4 and 5 show the above listed sources.

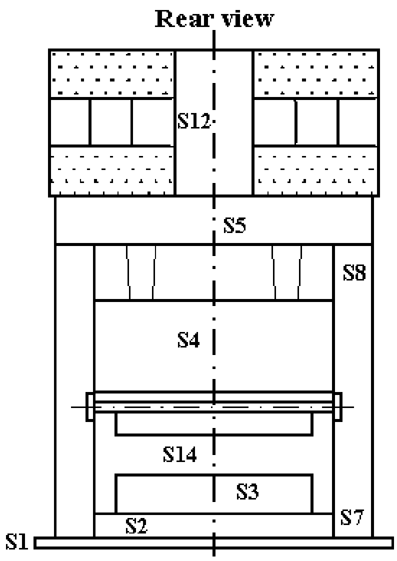

Figure 4: Sources at press rear face.

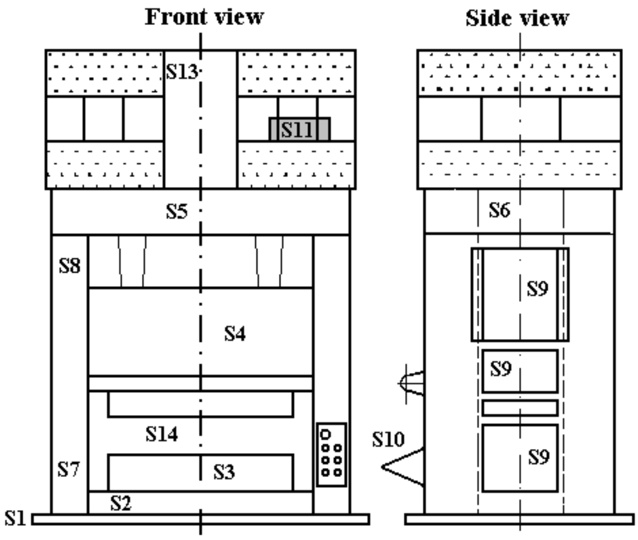

Figure 5: Sources at press front and side faces.

Different procedures were used to estimate the sound power radiated by the several press components. Measurements included space averaged floor vibration (S1), space averaged squared velocity of the several components (S2 to S10), sound intensity measurements of electric motor (S11) (ISO Standard, 1993), monitoring of sound pressure levels at several points distributed around the press, particularly near brake, clutch and gearbox (S12 to S14), (Azevedo, 2003).

The sound power emitted by a vibrating surface can be estimated by the equation (Beranek and Vér, 1992):

$$W_{rad} = \sigma_{rad} \; \rho_0 \; c_0 \, S \left\langle \bar{v}^2 \right\rangle \quad , \tag{1}$$

where σ_{rad} is the radiation efficiency, ρ_0 is the air density, c_0 the sound velocity in air, S the surface area and $\left\langle \bar{v}^2 \right\rangle$ the space averaged squared velocity.

The radiation efficiency values were obtained under simplified assumptions (Beranek and Vér, 1992), considering two basic approaches: for massive elements (like stamps) it was assumed the oscillating body hypothesis and for some plates (like parts of the columns) it was assumed the thick plate hypothesis. An example of radiation efficiency versus frequency curve is shown in Fig. 6, for the thick plates of the hammer, in one third octave center frequency values.

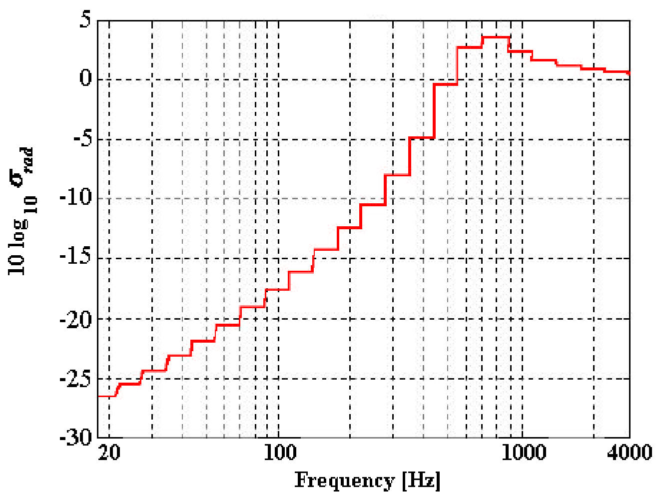

Figure 6: Radiation efficiency of the thick plates of the hammer.

Applying Eq. (1) it was possible to obtain the estimated one third octave band sound power spectra, shown in Figs. 7 and 8, for SPL_{1s} and impulsive SPL_{35ms} levels, respectively.

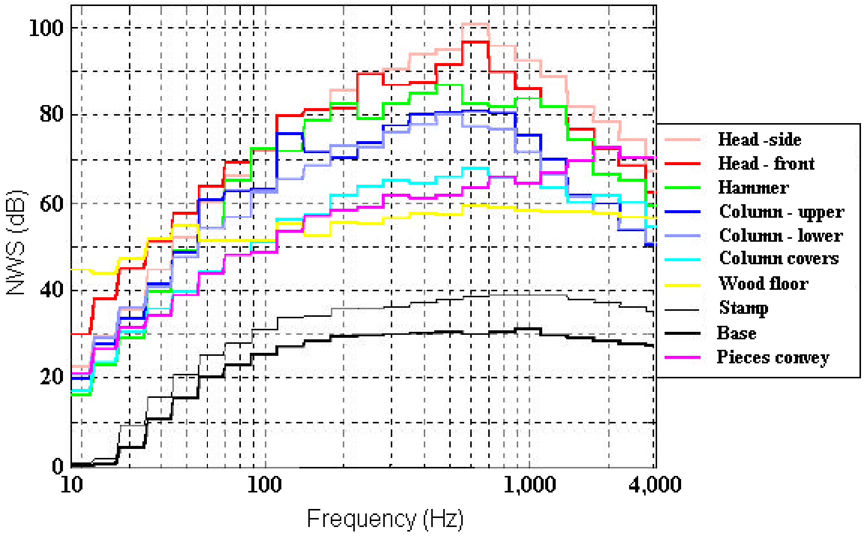

Figure 7: Sound power spectra of various sources, continuous noise (SPL_{1s}).

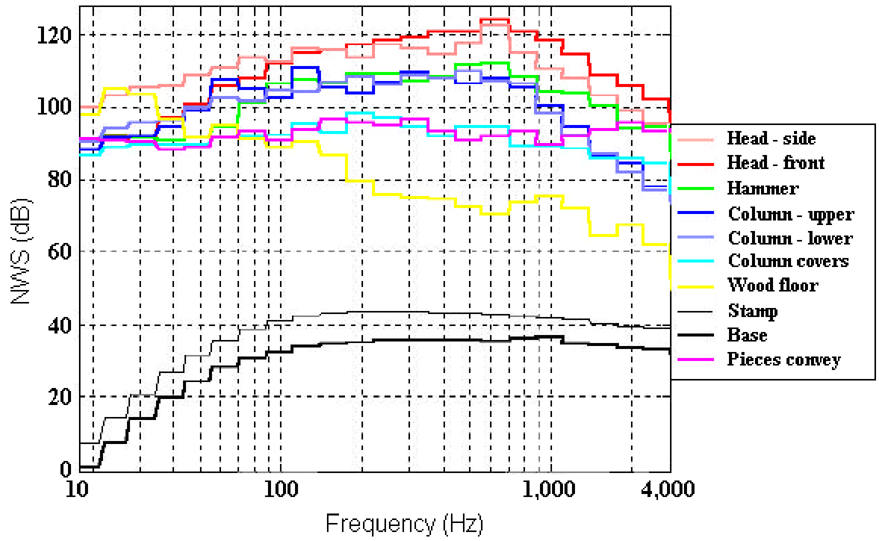

Figure 8: Sound power spectra of various sources, impulsive noise (SPL_{35ms}).

In order to estimate the sound pressure levels at operator's position, based on previous noise power levels, it was used the following equation (Beranek and Vér, 1992):

$$NPS(\theta) = NWS + 20 \log_{10} Q(\theta) - 20 \log_{10} r - 11 \quad , \tag{2}$$

where $NPS(\theta)$ is the resulting noise pressure level, NWS the noise power level, $Q(\theta)$ the directivity factor and r the distance between source and receiver. Under a simplified assumption, it was assumed that all sources were omni directional, so that the directivity factor is equals to unity, and so the term $20 \log_{10} Q(\theta)$ vanishes.

Table 3 presents the distance r (used in Eq. (2)) from the main sources to operator's position.

Figures 9 and 10 present the resulting global values of the noise sound levels at operator's position, referring to various sources, in terms of continuous and impact values.

Table 3: Assumed distances from sources to operator's position.

Sources	**Distances [m]**
Head frontal area	5.07
Head side area	5.05
Hammer	1.00
Column upper area	5.00
Column lower areas	1.50
Column covers	3.22
Pieces convey	1.80
Floor	1.00
Impact area (stamps)	1.00
Base	1.20
Clutch	5.87
Brake	5.87
Main electric motor	5.50

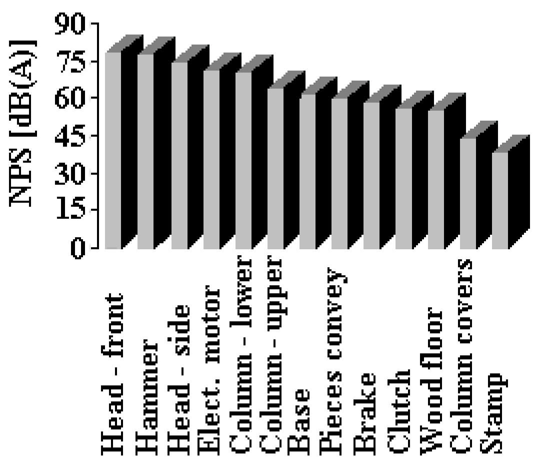

Figure 9: Noise pressure levels produced by the main noise sources, in equivalent form (1s averaging time).

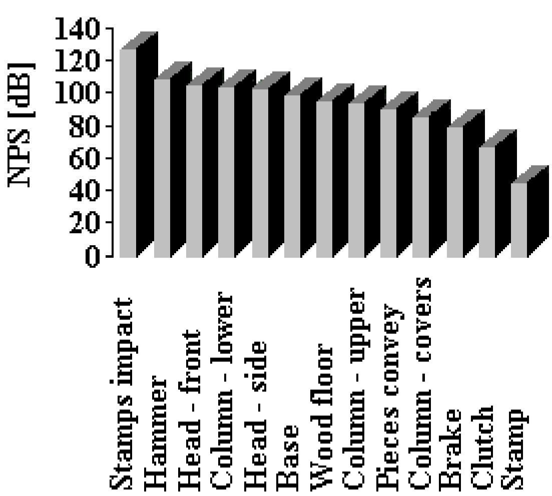

Figure 10: Noise pressure levels produced by the main noise sources, in impulsive form (35 ms averaging time).

5. Conclusions

Measurement of surface vibrations has proven to be an efficient procedure for the estimation of sound power radiation from structures using radiation efficiency values. It is expected, then, that this approach may also produce good results for other industrial machines and equipments.

The noise produced by eccentric presses is directly related to the impact of the hammer against the stamp. This event gives rise to high vibrations levels all over the press structure, resulting in high sound energy radiation.

This impact phase (C-D) and the following one (phase D-E), related to the material fracture, are the noisiest ones, and produce noise levels approximately 16 dB above the average level produced in all other phases.

The period just after the impact (phases E-F, F-G and G-H), which is characterized by residual vibrations and hammer ascent, presents an average noise level also high, about 8 dB higher than the levels corresponding to the phases (B-C and H-I), when occurs basically the movement of the hammer.

Head areas, both in front and side regions, are the main sources of continuous noise (SPL_{1s}). Next important sources, in this case, are the hammer and the electrical motor.

Hammer impact, material fracture and air expulsion are the most important sources of impact noise (SPL_{35ms}).

With regards to the frequency contents, the hammer impact produces mainly low frequency noise (88 Hz to 144 Hz). Upper components of the press radiate noise, after the hammer impact, in a range of frequencies slightly higher (238 Hz to 570 Hz). Finally, the stamps and the press base, responding to the hammer impact, produce noise at higher frequencies (1,000 Hz to 1,500 Hz).

One can also notice that noise levels for each individual component as identified and shown in Figs. 9 and 10 are in fairly good agreement with results shown in Tab. 2. Overall SPL_{35ms} are of the order of 120 dB and SPL_{1s} of the order of 100 dBA.

6. References

Stimpson, G. J., and Richards, E. J., 1985, “On the Prediction of Impact Noise, Part IX: The Noise from Punch Presses”, Journal of Sound and Vibration, vol. 103(1), pp. 43-81.

Azevedo, P. C., 2003, “Estudo da Geração de Ruído em uma Prensa Mecânica Excêntrica de 900 Toneladas”, M. Sc. Thesis, Mechanical Engineering Post-graduate Course, Federal University of Santa Catarina, Florianópolis, SC, Brazil, 116 p.

ISO 9614-1: 1993 – Acoustics – “Determination of Sound Power Levels of Noise Sources using Sound Intensity – Part 1: Measurement at discrete points”.

Beranek, L.L. and Vér, I.L, 1992, “Noise and Vibration Control Engineering: Principles and Applications”, Wiley Interscience, New York, USA, 816 p.